Kishal Bipin Tandel
23MS115
November 10, 2025

Report 5

Instructors:
Prof. Satyabrata Raj
Prof. Goutam D. Mukherjee

PH3105: Nuclear Physics Laboratory

Abstract

In this experiment, the operating characteristics and statistical behavior of radioactive decay were studied using a Geiger–Müller (GM) counter and a ^{22}Na γ-ray source. The operational plateau region of the GM tube was determined by measuring count rates at different applied voltages, and the distribution of recorded counts was analyzed to verify the Poisson nature of radioactive decay. The results confirmed the random, independent nature of nuclear disintegrations and demonstrated good agreement between the experimentally obtained standard deviation and the theoretical prediction based on counting statistics, thereby illustrating the inherent statistical uncertainties in radiation detection.

Contents

1. Introduction

The detection and quantification of nuclear radiation are central to experimental nuclear physics. Among several detectors, the Geiger–Müller counter is widely used for measuring the intensity of ionizing radiation due to its simplicity, robustness, and efficiency for α, β, and γ radiations. In this experiment, the GM counter is employed to investigate its operational characteristics and to study the random statistical behavior of radioactive decay events.

1.1 Aim

The aims of this experiment are:

1. To plot the operational characteristic curve of the GM counter and determine its operating voltage.
2. To study the statistical distribution of radioactive decay counts and verify the Poisson nature of counting statistics.

1.2 Apparatus and Materials

The experimental setup comprises the following main components, as per the PHYWE manual:

1. Para Nuclear Counter
2. Geiger–Müller tube (halogen-quenched type)
3. ^{22}Na γ-ray source
4. High-voltage supply (0–1500 V adjustable)
5. Data acquisition system / digital counter

1.3 Experimental Setup and ^{22}Na Source

The experimental set up and ^{22}Na source is shown in Figure 1.

Figure 1: Experimental setup (left) and ^{22}Na source (right)

2. Theory

2.1 Geiger–Müller Counter

2.1.1 Construction and Basic Principle

A schematic of the Geiger–Müller counter is shown in Figure 2. The instrument consists of a cylindrical metal tube acting as the cathode and a fine axial wire serving as the anode. The space between them is filled with a suitable low-pressure gas mixture—commonly argon mixed with a small percentage of an organic or halogen quenching agent. A potential difference of the order of 400–1000 V is applied between the electrodes through a large series resistor.

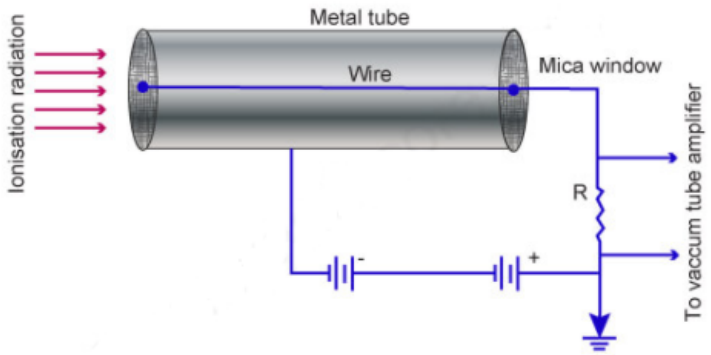

Figure 2: Schematic diagram of a Geiger–Müller counter setup.

When ionizing radiation passes through the gas, it knocks electrons from the gas atoms, creating primary ion pairs. If the applied voltage is sufficiently high, the freed electrons gain enough kinetic energy to ionize additional gas atoms, initiating a chain of collisions known as a Townsend avalanche. The total number of ions produced becomes extremely large—of order 10^9—providing a detectable electrical pulse.

2.1.2 Townsend Avalanche and Gas Amplification

The operation of the counter depends on the formation of Townsend avalanches within the gas. Even a single primary ion pair can trigger a full discharge. The liberated electrons accelerate toward the central wire where the electric field is strongest, repeatedly ionizing neutral atoms and creating successive generations of electrons. Because positive ions are massive, they drift slowly toward the cathode and contribute negligibly to further ionization. By the time the avalanche reaches the anode, the initial ionization has been amplified by many orders of magnitude, producing a pulse of nearly constant height irrespective of the energy of the incoming particle.

2.1.3 Operating Regions and Plateau Characteristic

A minimum potential difference is required across the tube before the avalanche process begins. Below this *starting voltage*, the number of ions collected is too small for reliable pulse detection. As the voltage is increased, the pulse height grows and eventually becomes independent of the initial ionization, marking the onset of the Geiger region. The number of pulses per second for a constant source then remains practically constant even as voltage increases further. This behavior is illustrated in Figure 3, where the count rate is plotted versus applied voltage.

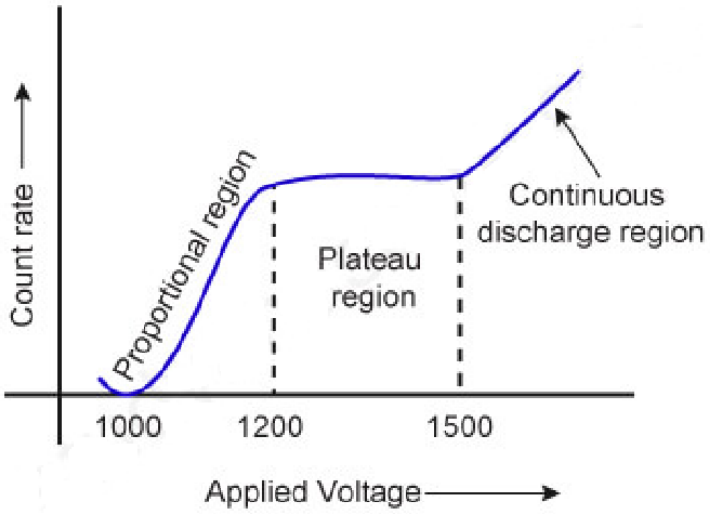

Figure 3: Characteristic curve of GM Tube

The nearly horizontal portion of the curve, called the *plateau*, represents the stable operating range of the counter. Its slope in a good tube is typically 2–5% per 100 V over a region of about 200 V. The *starting voltage* marks the beginning of observable counting, while the *threshold voltage* defines the point at which Geiger action becomes uniform. The counter is usually operated near the midpoint of the plateau to minimize sensitivity to small voltage fluctuations. Operating at a voltage above the threshold is referred to as applying an *over-voltage*. As the voltage approaches the continuous-discharge region, the shielding effect of the positive ion sheath breaks down and the counter may discharge continuously, which must be avoided.

2.1.4 Quenching and Pulse Recovery

Each avalanche leaves behind a large number of positive ions near the anode, which can release secondary electrons upon striking the cathode and thereby cause spurious afterpulses. To prevent this, the fill gas includes a small proportion of a quenching vapor (such as alcohol or halogen compounds) that absorbs the energy of excited ions and neutralizes them without producing new electrons.

When the avalanche reaches the wire, the sudden influx of positive ions locally reduces the electric field, lowering the effective potential difference and terminating the discharge. The high-value resistor connected in series with the anode then allows the charge on the central wire to leak off gradually, restoring the initial field and rendering the tube ready for the next event. If the resistor were not of order $10^9\ \Omega$, a continuous discharge would develop. The recovery time of the counter is determined by the RC time constant of the anode circuit, typically around

$$RC \approx (10^9\ \Omega) \cdot (10^{-11}\ \mathrm{F}) = 10^{-2}\ \mathrm{s}$$

This implies a *dead time* of approximately 0.01 s during which the counter cannot record another event. Any two ionizing events separated by less than this interval will merge, and only one pulse will be registered. The corresponding maximum count rate without severe losses is therefore on the order of 10^2 counts per second.

2.2 Counting Statistics

2.2.1 Nature of Radioactive Decay

Radioactive decay is an inherently random process governed by the principles of quantum mechanics. Each nucleus in a radioactive sample has a constant probability per unit time of decaying, independent of the behavior of other nuclei. Consequently, the number of decays, or counts recorded by a detector in any fixed time interval, fluctuates randomly about a mean value. The study of these fluctuations, known as counting statistics, provides direct experimental evidence for the stochastic nature of radioactive decay and establishes a quantitative basis for estimating uncertainties in nuclear measurements.

2.2.2 Poisson Distribution and Fundamental Relations

If the mean number of counts recorded in a fixed time interval is $\bar{n}$, then the probability of observing exactly n counts is given by the Poisson distribution,

$$P(n) = \frac{e^{-\bar{n}}\,\bar{n}^n}{n!}$$

This distribution is valid for independent random events that occur with a constant average rate, as is the case for nuclear disintegrations and detection events in a Geiger–Müller counter. A defining property of the Poisson distribution is that its variance equals its mean, $\sigma^2 = \bar{n}$, implying that the statistical uncertainty in a single counting measurement is $\sigma = \sqrt{\bar{n}}$. The relative uncertainty thus decreases with increasing mean count as $\sigma/\bar{n} = 1/\sqrt{\bar{n}}$, demonstrating the square-root law that governs the precision of radioactive measurements. This simple but powerful relation also provides the basis for estimating measurement errors in all nuclear counting experiments.

2.2.3 Central Limit Theorem and Gaussian Approximation

As the number of observations increases, the statistical behavior of the count distribution transitions from purely Poissonian to approximately Gaussian. This is a direct consequence of the *Central Limit Theorem (CLT)*, which states that the sum (or average) of a large number of independent random variables—each drawn from any distribution with finite variance—tends toward a normal (Gaussian) distribution, regardless of the original distribution's shape. In the context of radioactive decay, each individual disintegration is an independent random event following the Poisson law. When a large number of such events are recorded, the combined distribution of counts per interval approaches a Gaussian form centered on the mean $\bar{n}$.

Mathematically, for large $\bar{n}$ (typically $\bar{n} > 30$), the Poisson distribution can be approximated by the Gaussian distribution,

$$P(n) \approx \frac{1}{\sqrt{2\pi\bar{n}}} \exp\left[-\frac{(n-\bar{n})^2}{2\bar{n}}\right]$$

which is symmetric about the mean and characterized by a standard deviation $\sqrt{\bar{n}}$. The CLT thus provides the theoretical justification for using Gaussian statistics in the analysis of large-count nuclear measurements and supports the use of least-squares and chi-squared fitting methods.

2.2.4 Reduced Chi-Squared Test for Gaussian Fit

To quantitatively evaluate how well the experimentally observed binned distribution of counts follows the Gaussian form predicted by the Central Limit Theorem, the *reduced chi-squared test* was

employed. This test compares the observed frequency of counts in each bin with the corresponding expected frequency from the fitted Gaussian model and provides a dimensionless measure of the goodness of fit.

Since radioactive decay follows Poisson statistics, the statistical uncertainty in each observed frequency is given by

$$\sigma_i = \sqrt{O_i}$$

where O_i represents the number of counts (frequency) observed in the i^{th} bin. The chi-squared statistic, which quantifies the deviation between observation and theory, is then defined as

$$\chi^2 = \sum_{i=1}^{k} \frac{(O_i - E_i)^2}{\sigma_i^2} = \sum_{i=1}^{k} \frac{(O_i - E_i)^2}{E_i}$$

Here, E_i represents the expected frequency in the i^{th} bin, obtained from the Gaussian model.

Since the Gaussian model contains two fitted parameters—the mean count $\bar{n}$ and the standard deviation σ—the number of degrees of freedom is given by

$$\nu = k - p - 1 = k - 3$$

where $p = 2$ corresponds to the fitted parameters and one additional degree of freedom is lost because the expected frequencies are normalized such that $\sum_i E_i = N_{\text{tot}}$. The *reduced chi-squared statistic* is then expressed as

$$\chi^2_\nu = \frac{\chi^2}{\nu} = \frac{1}{\nu} \sum_{i=1}^{k} \frac{(O_i - E_i)^2}{E_i}$$

The expected frequencies E_i are obtained from the fitted Gaussian probability density function

$$f(n) = \frac{1}{\sqrt{2\pi\sigma^2}} \exp\left[-\frac{(n-\bar{n})^2}{2\sigma^2}\right]$$

through the relation

$$E_i = N_{\text{tot}} \int_{n_i}^{n_i+\Delta n} f(n)\, dn$$

which, for small bin widths Δn, may be approximated as

$$E_i \approx N_{\text{tot}}\, f(n_i)\, \Delta n$$

A reduced chi-squared value of $\chi^2_\nu \approx 1$ indicates that the deviations between observed and expected frequencies are consistent with random statistical fluctuations, confirming that the data conform to the Gaussian distribution predicted by the Central Limit Theorem. If $\chi^2_\nu \gg 1$, the observed fluctuations are larger than statistically expected, which may suggest inappropriate binning, unaccounted systematic errors, or detector instabilities. Conversely, $\chi^2_\nu \ll 1$ indicates that the data have been over-fitted or that the uncertainties are overestimated.

2.3 Decay Scheme of ^{22}Na

Sodium-22 (^{22}Na) is a radioactive isotope with a half-life of approximately 2.6 years. It decays predominantly by positron emission (β^+-decay) and, to a smaller extent, by electron capture (EC). The two competing decay modes are as follows:

1. Positron emission (β^+-decay):

$$^{22}_{11}\mathrm{Na} \longrightarrow {}^{22}_{10}\mathrm{Ne}^* + e^+ + \nu_e$$

2. Electron capture (EC):

$$^{22}_{11}\mathrm{Na} + e^- \longrightarrow {}^{22}_{10}\mathrm{Ne}^* + \nu_e$$

In both processes, the daughter nucleus $^{22}_{10}\mathrm{Ne}^*$ is produced in an excited state and subsequently de-excites to its ground state by emitting a characteristic γ-ray photon of energy

$$E_\gamma = 1.275 \text{ MeV}$$

The excited-state transition can thus be represented as

$$^{22}_{10}\mathrm{Ne}^* \longrightarrow {}^{22}_{10}\mathrm{Ne} + \gamma(1.275 \text{ MeV})$$

The emitted positron (e^+) from β^+-decay interacts with an ambient electron (e^-) in the surrounding material and annihilates, producing two back-to-back γ-ray photons of energy

$$e^+ + e^- \longrightarrow 2\gamma(0.511 \text{ MeV each})$$

Hence, every positron emission event produces two annihilation photons of 0.511 MeV each and one prompt nuclear γ photon of 1.275 MeV, resulting in three distinct γ components in the decay radiation field.

3. Operational Characteristic Curve of GM Tube

3.1 Observation Table

We placed the ^{22}Na source in slot 4 and acquired two readings for 30 s each at different HV values. We have listed the raw measurements in Table 1.

Sr. No.	High Voltage (V)	Count 1 (per 30 s)	Count 2 (per 30 s)	Mean Count (per 30 s)
1	0	0	0	0.0
2	50	0	0	0.0
3	100	0	0	0.0
4	150	0	0	0.0
5	200	0	0	0.0
6	250	0	0	0.0
7	270	0	0	0.0
8	290	0	0	0.0
9	310	0	0	0.0
10	330	0	0	0.0
11	350	358	352	355.0
12	400	357	361	359.0
13	450	380	382	381.0
14	500	369	384	376.5
‘15	550	393	398	395.5
16	600	382	343	362.5
17	650	352	379	365.5
18	700	387	401	394.0
19	750	368	377	372.5
20	800	412	400	406.0
21	850	407	390	398.5
22	900	414	404	409.0
23	950	532	559	545.5
24	970	576	566	571.0
25	990	652	674	663.0
26	1010	748	727	737.5
27	1030	835	833	834.0
28	1050	891	902	896.5

Sr. No.	High Voltage (V)	Count 1 (per 30 s)	Count 2 (per 30 s)	Mean Count (per 30 s)
29	1070	1045	1083	1064.0
30	1090	1297	1298	1297.5
31	1110	1445	1469	1457.0
32	1120	1714	1741	1727.5

Table 1: High Voltage (V) vs. Count (per 30 s)

3.2 Characteristic Curve of GM Tube

On plotting Count (per 30s) vs. High Voltage (V) from Table 1, we get the characteristic curve of GM counter as shown in Figure 4.

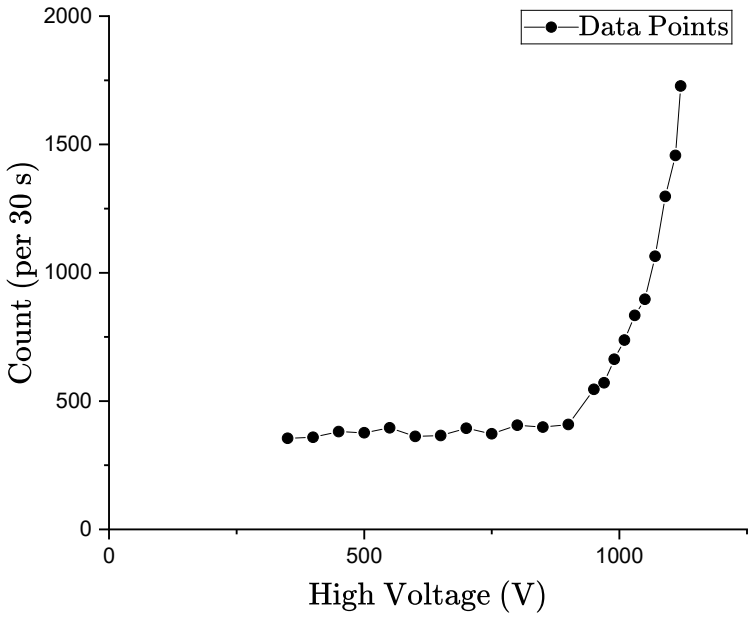

Figure 4: Characteristic Curve of GM Tube

3.3 Discussion

The variation of the observed count rate with applied high voltage (HV) across the Geiger–Müller (GM) tube was studied to determine the threshold voltage, the plateau region, and the onset of continuous discharge. The measured count rates for successive HV settings (each recorded over an interval of 30 s) are presented in Table 1 and plotted in Figure 4.

At low voltages (below 300 V), the electric field inside the GM tube is insufficient to produce Townsend avalanches, and consequently, no detectable pulses are observed. As the voltage increases beyond approximately 350 V, the count rate begins to rise sharply, indicating the *threshold volt-*

age—the minimum potential at which the primary ionization electrons acquire sufficient energy to initiate secondary avalanches. For the present GM tube, the threshold voltage is approximately

$$V_{\text{th}} \approx 350 \text{ V}$$

Between about 450 V and 850 V, the count rate remains nearly constant with increasing voltage, forming the characteristic *plateau region* of the GM counter. In this region, each ionizing event results in a full discharge pulse independent of the energy or number of primary ion pairs created. The count rate changes by less than about 2–3% per 100 V, which indicates excellent operating stability. The slope of the plateau determines the quality of the counter; a smaller slope implies greater immunity to voltage fluctuations.

The *recommended operating voltage* is chosen near the middle of this plateau to ensure reliable operation even if the supply voltage drifts slightly. From the present data, the plateau midpoint occurs near

$$V_{\text{op}} \approx 600 \text{ V} - 650 \text{ V}$$

At this voltage, the GM tube operates in the true Geiger region—producing uniform pulses that can be accurately counted without risk of incomplete discharges.

Beyond about 900 V, a rapid increase in count rate is observed, rising from 409 counts at 900 V to more than 1700 counts at 1120 V. This marks the *onset of continuous discharge or breakdown region*, where the positive ion sheath around the anode can no longer quench the discharge effectively. In this region, spurious pulses and continuous conduction dominate, rendering the counter unusable for quantitative measurements.

In summary, the GM counter exhibits:

$$\begin{aligned} \text{Threshold voltage:} &\quad V_{\text{th}} \approx 350 \text{ V} \\ \text{Plateau region:} &\quad 450 \text{ V} \leq V \leq 850 \text{ V} \\ \text{Operating voltage:} &\quad V_{\text{op}} \approx 600 \text{ V–}650 \text{ V} \\ \text{Onset of breakdown:} &\quad V_{\text{bd}} \approx 900 \text{ V} \end{aligned}$$

These results confirm the expected characteristics of a well-behaved GM counter, demonstrating distinct operating regions and an extended plateau suitable for stable radiation detection.

4. Counting Statistics of Radioactive Decay

4.1 Observation Table

We have set high voltage as 600 V for our operating voltage and placed the ^{22}Na source in slot 3. We acquired 300 readings for 30 s each. We have listed the count and the corresponding frequency in the following Table.

Count	Frequency	Count	Frequency	Count	Frequency	Count	Frequency
505	1	542	3	566	4	591	2
508	1	543	3	567	4	592	3
509	1	544	7	568	5	593	2
512	1	545	2	569	5	594	2
515	1	546	5	570	3	596	3
516	1	547	5	571	5	597	2
519	1	548	2	572	4	598	3
521	3	549	5	573	6	599	1
522	2	550	5	574	4	600	2
524	2	551	8	575	4	601	4
525	1	552	5	576	3	603	1
526	1	553	4	577	3	605	1
527	1	554	6	578	3	606	1
528	2	555	4	579	5	607	2
530	2	556	4	580	3	609	3
531	2	557	6	581	7	611	1
532	2	558	5	583	5	613	1
533	2	559	7	584	5	619	1
535	2	560	10	585	3	621	1
537	2	561	6	586	5	622	1
538	1	562	3	587	1	625	2
539	4	563	5	588	3	626	1
540	3	564	4	589	4	630	1
541	3	565	4	590	5		

Table 2: Count vs. Frequency

4.2 Bin vs. Reduced Chi-Squared χ^2_ν

Using the data from the count–frequency table, the distribution was fitted with a Gaussian function, and the corresponding reduced chi-squared (χ^2_ν) values for different bin widths were computed using *OriginPro Graphing and Analysis Software*. The results are listed in the following table:

Bin	χ^2_ν	Bin	χ^2_ν	Bin	χ^2_ν	Bin	χ^2_ν	Bin	χ^2_ν	Bin	χ^2_ν	Bin	χ^2_ν	Bin	χ^2_ν
1	0.61	3	0.73	5	0.71	7	0.83	9	0.79	11	1.11	13	1.02	15	0.81
2	0.53	4	0.49	6	0.78	8	0.71	10	0.77	12	1.02	14	0.88	16	0.69

Table 3: Bin vs. χ^2_ν

4.3 Composite Plot

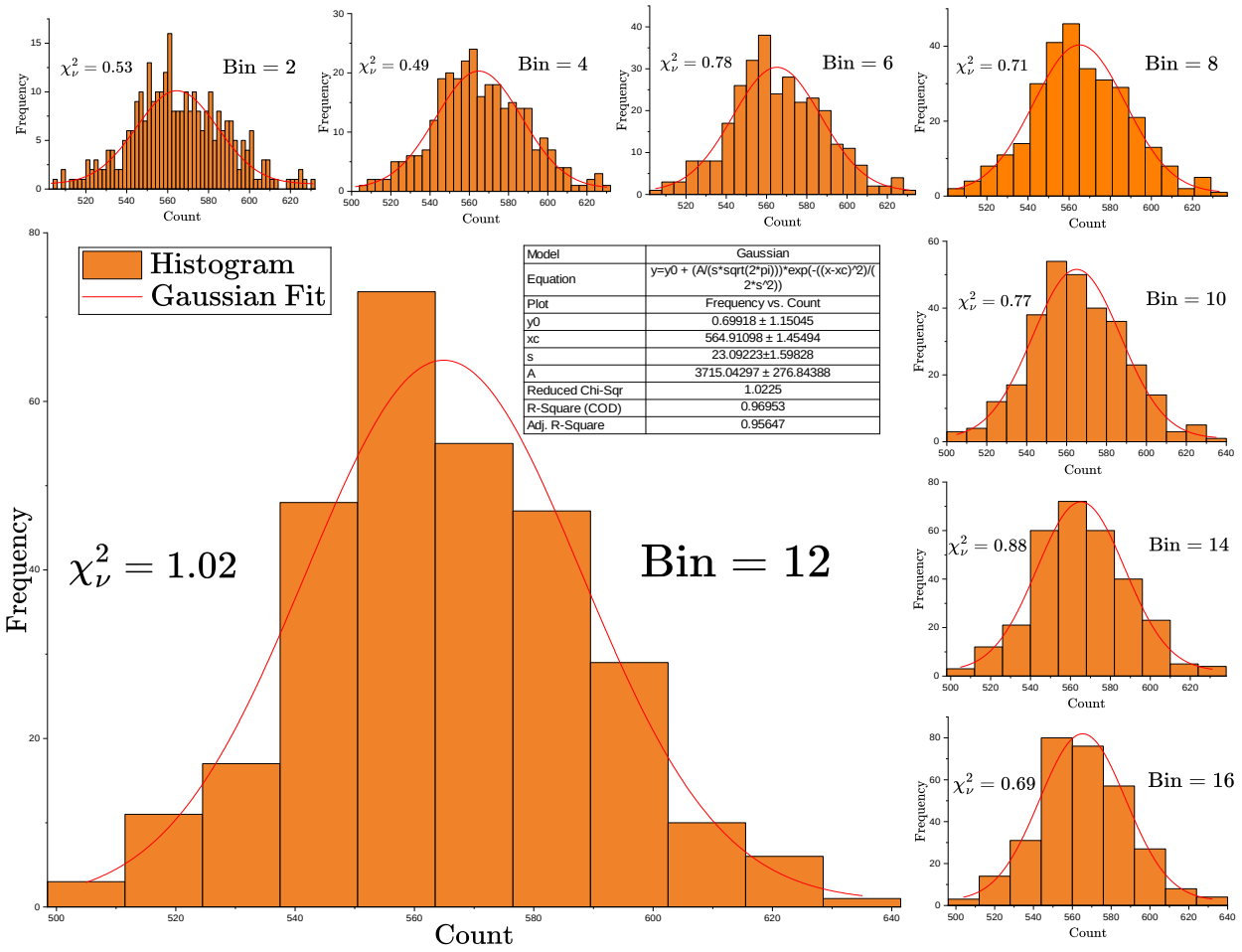

Figure 5: Composite plot showing Gaussian fits to the experimental count distributions for varying bin widths. The central plot corresponds to the binning configuration with reduced chi-squared value closest to unity ($\chi^2_\nu = 1.02$), indicating the optimal agreement with the Gaussian model predicted by counting statistics. The subplots display other bin widths for comparison, demonstrating how the goodness of fit varies with bin size.

4.4 Discussion

The measured count data exhibit the statistical fluctuations characteristic of radioactive decay. Over 300 readings, each taken for a fixed interval of 30 s at an operating voltage of 600 V, the counts were observed to vary randomly around a mean value of approximately 565 counts per interval. This randomness arises from the inherent probabilistic nature of nuclear disintegrations, each decay being an independent event. Since the mean count rate is relatively large, the distribution of counts is expected to follow a Gaussian form according to the Central Limit Theorem, which describes the normal approximation to the Poisson distribution for large $\bar{n}$.

To examine this behavior quantitatively, the experimental data were grouped into histograms using a range of bin widths, denoted as "bin = 1", "bin = 2", ..., "bin = 16". For each binning configuration, the count–frequency distribution was fitted with a Gaussian curve, and the reduced chi-squared value χ^2_ν was calculated to assess the goodness of fit. The computed values of χ^2_ν, listed in Bin vs. χ^2_ν Table, vary between approximately 0.5 and 1.1, demonstrating generally good agreement between experimental data and the Gaussian model. Notably, the configurations for bin = 12 and bin = 13 both yield $\chi^2_\nu = 1.02$, indicating that these bin widths provide the most statistically consistent fits to the expected Gaussian distribution.

In the composite plot (Figure 5), the central large plot corresponds to one of these optimal configurations, while the surrounding subplots display histograms for other bin widths. It is observed that for smaller bin widths, the histogram appears noisy and irregular due to significant statistical fluctuations within each narrow bin, leading to larger uncertainties in the frequencies and a less stable fit. As the bin width increases, the histogram becomes smoother, and χ^2_ν approaches unity. Beyond the optimal range, the histogram becomes overly coarse, reducing the number of degrees of freedom and producing an artificially small χ^2_ν. The occurrence of nearly identical χ^2_ν values for bin = 12 and 13 shows that a moderate variation in bin width does not significantly affect the fit quality once statistical equilibrium is reached.

For the best-fit configuration, the Gaussian fit parameters were found to be $\bar{n} = 564.91 \pm 1.45$ and $\sigma = 23.09 \pm 1.60$, giving $\chi^2_\nu = 1.02$ and $R^2 = 0.97$. These values confirm that the observed distribution closely follows a normal curve centered near the expected mean count. The experimental standard deviation σ is in very good agreement with the theoretical Poisson value $\sqrt{\bar{n}} \approx 23.77$, indicating that the observed fluctuations are consistent with counting statistics. Minor deviations could arise from experimental factors such as detector dead time, voltage instability, background radiation, or electronic noise in the GM counter circuit.

The near-Gaussian behavior of the count data and the optimal $\chi^2_\nu \approx 1$ verify the random, independent nature of nuclear disintegrations and validate the use of Gaussian statistics for describing counting experiments at high mean rates. This experiment therefore successfully demonstrates one of the fundamental results of nuclear statistics: the convergence of Poisson-distributed radioactive decay events toward a Gaussian distribution as the number of counts becomes large.

5 Sources of Error

5.1 Systematic Errors

1. **Dead Time of GM Counter:** The detector cannot record a new event immediately after one pulse, leading to undercounting at higher rates.

2. **Voltage Instability:** Small fluctuations in high voltage affect the gas amplification and,

consequently, the count rate.

3. **Background Radiation:** Variations in environmental radiation cause a steady offset in measured counts.
4. **Geometric Misalignment:** Small changes in the relative positioning of source and detector alter the detection probability.
5. **Threshold and Electronics Drift:** Improper or drifting discriminator levels may include spurious pulses or miss valid ones.

5.2 Random Errors

1. **Statistical Nature of Decay:** Radioactive decay follows Poisson statistics, giving rise to random fluctuations in counts.
2. **Electronic Noise:** Random noise in the detector or counting circuit introduces small unpredictable variations.
3. **Finite Sampling:** Only a limited number of readings (300 in this case) were taken, giving rise to statistical uncertainty in the mean and standard deviation.
4. **Binning Effects:** Grouping counts into bins introduces small random variations between adjacent bins.

6. Results

Part I — Operational Characteristic Curve of GM Tube:

1. The plateau region of the GM counter was observed between 450 V and 850 V.
2. The slope of the plateau was approximately 3% per 100 V, indicating good counter stability.
3. The operating voltage for further measurements was chosen as the midpoint of the plateau, i.e., 600 V.

Part II — Counting Statistics of Radioactive Decay:

1. A total of 300 readings, each over 30 s, were recorded at 600 V using a ^{22}Na source.
2. The counts ranged from 505 to 630 per 30 s.
3. The mean count and standard deviation from the Gaussian fit for the best-fit configuration were:
$$\bar{n} = 564.91 \pm 1.45, \quad \sigma = 23.09 \pm 1.60$$
4. The experimental standard deviation σ is in very good agreement with the theoretical Poisson value $\sqrt{\bar{n}} \approx 23.77$, indicating that the observed fluctuations are consistent with counting statistics.
5. The best fit was obtained for Bin = 12, with a reduced chi-squared value:
$$\chi^2_\nu = 1.02$$
6. The distribution of counts followed a Gaussian curve centered around the mean, confirming the expected statistical behavior of radioactive decay.

7 Conclusion

The experiment successfully demonstrated the operational behavior of a Geiger–Müller (GM) counter and the statistical nature of radioactive decay. From the characteristic curve, the threshold voltage was found to be approximately $V_{\text{th}} \approx 350$ V, and the plateau region extended from 450 V to 850 V with a slope of about 3% per 100 V, indicating good counter stability. The operating voltage of 600–650 V provided a region of reliable and reproducible counting.

In the second part of the study, the statistical analysis of counts from a ^{22}Na source confirmed the expected Poisson behavior of radioactive decay. The experimentally obtained mean count ($\bar{n} = 564.9$) and standard deviation ($\sigma = 23.1$) were in close agreement with the theoretical prediction $\sqrt{\bar{n}} \approx 23.8$. The reduced chi-squared value ($\chi^2_\nu = 1.02$) further verified that the observed distribution followed a Gaussian form, consistent with the Central Limit Theorem for large count numbers.

Hence, the experiment validated two key aspects of nuclear counting: (i) the stable operating characteristics of a GM tube, and (ii) the inherently random yet statistically predictable nature of radioactive decay events.

Future Scope and Improvements

- **Dead Time Correction:** Implement electronic dead-time correction or use a GM tube with shorter recovery time to minimize undercounting at high activity levels.
- **Background Subtraction:** Record background radiation separately and subtract it from total counts to improve measurement accuracy.
- **Extended Source Study:** Repeat the experiment using other isotopes such as ^{137}Cs or ^{90}Sr to compare counting statistics across different decay modes.
- **Environmental Control:** Maintain constant temperature and shielding conditions to minimize external effects like voltage drift or background fluctuations.

These improvements would enhance both the precision and reliability of future measurements and allow a more comprehensive study of detector characteristics and counting statistics.

References

1. D. Halliday, R. Resnick, and J. Walker, *Fundamentals of Physics*, 11th ed., Wiley, 2018.
2. K.S. Krane, *Introductory Nuclear Physics*, Wiley, 1988.
3. G.F. Knoll, *Radiation Detection and Measurement*, 4th ed., Wiley, 2010.
4. J.M. Blatt and V.F. Weisskopf, *Theoretical Nuclear Physics*, Springer, 1979.
5. A. Beiser, *Concepts of Modern Physics*, 6th ed., McGraw–Hill, 2003.
6. J. R. Lamarsh and A. J. Baratta, *Introduction to Nuclear Engineering*, 3rd ed., Prentice Hall, 2001.
7. J. Burcham and M. Jobes, *Nuclear and Particle Physics*, 2nd ed., Pearson, 2014.